Kinetics of Liquid Film Disintegration at "Bag" Mode of Drop Breakup

A. G. Girin [1*], Ye. A. Ivanchenko [2]
[1] Odessa National Maritime University, [2] Odessa State Institute of Finance, Odessa, Ukraine
club21@ukr.net and jeki1@rumbler.ru

Abstract

The process of liquid film disintegration at "bag" mode of drop breakup is connected with mechanism of hydrodynamic instability of Kelvine – Helmholtz type under action of air stream. After initial film rupture, caused by instability, behavior of liquid film is governed by two factors: further action of instability mechanism near the streamlined film edge and liquid gathering there into moving toroidal roller by the action of surface tension forces. When characteristic time of first process is greater, than of the second one, the surface tension grasps significant amount of liquid into roller before unstable disturbance shakes it off from the edge. Therefore, the diameter of the roller and the sizes of shaken-off droplets are greater than thickness of the film. Solution of a simplest problem about instability of liquid layer in gas flow was applied to determine the characteristic size and time of dominant unstable disturbance. At simplest assumptions (media are ideal, film is plane, liquid roller has a form of torus) the ordinary differential equation of motion of torus under action of surface tension forces and reactive forces is derived and laws of torus motion and of its radius changing in time are calculated. Taking into account simultaneously both mechanisms of unstable shaking-off and of the liquid roller growth, the main regularities of film disintegration kinetics have been calculated: histories of roller radius and of quantity of shaken-off droplets, moments of their generation and the period of full film disintegration.

Introduction

The interest to drop breakup phenomena exists for a long time in a connection with various processes, which perform in energetic machines (rocket, diesel and gasoline engines), in heterogeneous detonation, in fire suppression, in testing aircraft for high-speed interaction with cloud drops, etc. In many of these processes drop breakup occurs as well-established experimentally "bag"-mode, when drop deforms initially into a thin liquid disk, which then sags at the center and blows-out into vast bag (see, for example, [1]–[4]). The disintegration itself consists in rupture of thin bag film and then of massive rim, which generates aerosol cloud of fine droplets. Sizes of appeared daughter droplets, moments and location of their generation are the main parameters of breakup process, as they determine further preparing of homogeneous combustible mixture (motion, evaporation and fuel vapours mixing with oxidizer), which is of most importance in engine performance. To obtain the reliable information, valid for a wide range of conditions, we need to discover the mechanisms of bag and rim formation and their rupture, which would give the base regularities of these processes.

Many of papers were concerned mechanism of bag blowing-out: simple sagging of central part of liquid disk under action of pressure head at stagnation point [5], [6]; critical stage of deformation [3], [7]; action of air vortex [8], were enlisted as possible reasons. But none of these hypotheses were elaborated properly to be able to predict theoretically mentioned above parameters of the process.

It is supposed in present paper, that bag and bag-with-a-stamen blowing-out is caused by action of unstable aperiodic disturbances of Rayleigh – Taylor type. This hypotheses was declared in [9] and was developed in one of the paper submitted to 12th ICLASS [10]. It helps us to estimate below the important values of the liquid mass in the rim and the thickness of the bag film, which are necessary to evaluate sizes of daughter droplets. The model of liquid film disintegration is developed below, which describes two stages of the process – initial perforation of the film and further dynamics of the expanding hole, which is accompanied by film splashing. Many of experimental observations (fig. 1, which is taken from paper [1]), show, that prior to film disintegration a small dark spot is surrounded by concentric rings on the film. As the authors [1] have noted, this details in the bag structure may be the beginning of rupture of bag film. It is naturally to suppose in this connection, that the side of thin liquid film, which is exposed to streamlining gas stream, undergoes action of hydrodynamic instability of Kelvine – Helmholtz type and in the most preferable spot on the bag surface the unstable disturbance begins to grow at first, as fig. 1 snipes. Two competing mechanisms are enlisted in present paper as responsible for the dynamic behaviour of film after initial hole appearance: conservative action of surface tension at the film edge,

* Corresponding author: club21@ukr.net

which grasp the liquid into the roller, and simultaneous continuous destructive action of instability, which shakes off this roller in a form of droplets (fig. 2 taken from paper [11]). Hence, the problem of film disintegration is divided on the two parts: it is necessary to describe the dynamics of roller motion and growth, and to obtain parameters of dominant unstable disturbance on film surface, that shakes the roller off.

Figure 1 Wave structure on the bag film at the moment prior to film perforation

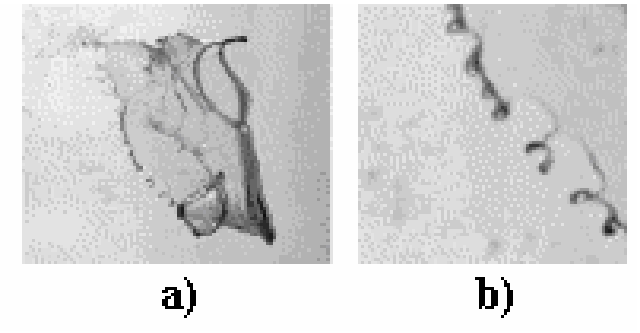

Figure 2 Roller moving and splashing of the bag film (a); fragment of film edge (b) [11]

Instability of Liquid Film

Evidently, the investigation of liquid film instability in the case considered can be carried out at a simplest formulation, applying small perturbation technique for inviscid fluids. As film thickness is much smaller than bag diameter D_b, let's consider the side part of film as a plane layer of thickness b (domain II, $0<y<b$, fig. 3), which is streamlined by gas flow over bag (domain III, $y>b$), while the gas inside bag (domain I, $y<0$) is at rest. For small disturbances of layer surfaces $y=0$, $y=b$ of "running-wave" type $\varepsilon_{1,2}=E_{1,2}\exp(ihx-i\omega t)$ the disturbances of velocity components U'_x, U'_y and pressure p' must satisfy to linearized equations of incompressible fluid. By reducing the boundary-value problem to the eigenvalue problem in usual way, we obtain the dispersion relation between disturbance frequency $z=\omega b/U_g$ and its wavelength $H=2\pi b/\lambda$:

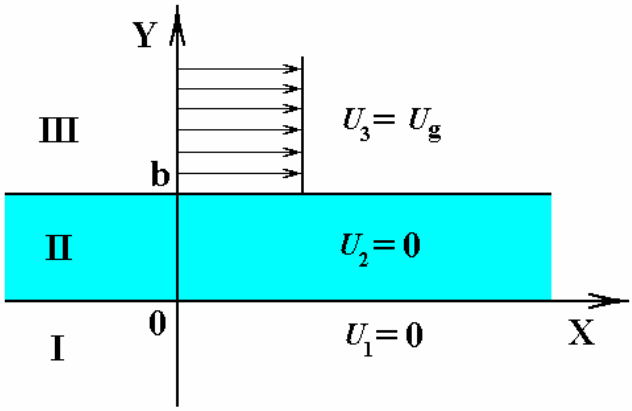

Figure 3 Scheme of liquid film

$$z^4\left(A_1+\Sigma A_2+\Sigma^2 A_3\right)+z^3\left(A_4\Sigma+A_5\Sigma^2\right)+z^2\left(A_6\Sigma+A_7\Sigma^2\right)+zA_8\Sigma^2+A_9\Sigma^2=0, \qquad 1)$$

where $\Sigma=\alpha/\mathrm{We_f}\ll 1$, $\alpha=\rho_g/\rho_l$ is gas-liquid density ratio, U_g is velocity of gas past drop, $\mathrm{We_f}=\rho_g b U_g^2/\sigma$ – Weber number for film, A_{1-9} are the functions of H, $\mathrm{We_f}$, which are given in **Appendix**. Consider solution of (1) in a form of asymptotic series $z=\Sigma^k\left(S_0+S_1\Sigma^{k_1}+\ldots\right)$ with respect to small parameter Σ. Substituting into (1) and equalizing terms with the same powers, we reveal the existence of unstable root of the form:

$$z=\Sigma^{0.5}S_0+\Sigma S_1+\ldots, \qquad with \quad k=k_1=0.5, \qquad 2)$$

where

$$S_0=iH\left(\frac{\left((2H-\mathrm{We_f})^2(1+e^{-2H})^2+4H(\mathrm{We_f}-H)(1-e^{-2H})^2\right)^{0.5}-(2H-\mathrm{We_f})(1+e^{-2H})}{2(1-e^{-2H})}\right)^{0.5}, \quad S_1=-\frac{A_8+A_4S_0^2}{4A_1S_0^2+2A_7}. \qquad 3)$$

There exists the fastest disturbance in the range of instability $0<H<\mathrm{We_f}$, which is of prime importance as its amplitude grows faster than all others grow and namely this dominant disturbance can be realized on non-linear stage of development. For the liquid film it would mean the perforation and formation of a hole of radius $r_0 \sim \lambda_\mathrm{m}$ in a film. By applying extremum condition $\partial\omega/\partial\lambda=0$ in the range of instability $0<H<\mathrm{We_f}$ we have obtained transcendental equation with respect to wavenumber H_m of dominant disturbance in the form

$$2(1-e^{-2H_\mathrm{m}})\left(\frac{W_1}{2W_2}-W_3\right)-4\left(W_2-H_\mathrm{m}^2(2H_\mathrm{m}-\mathrm{We_f})(1+e^{-2H_\mathrm{m}})\right)e^{-2H_\mathrm{m}}=0\,, \qquad 4)$$

where W_1, W_2, W_3 are the functions of $\mathrm{We_f}, H_\mathrm{m}$, given in **Appendix**. Making calculus, we have obtained values of wavelength $L_\mathrm{m}(\mathrm{We_f})=\lambda_\mathrm{m}(\mathrm{We_f})/b$ and characteristic time interval $T_\mathrm{e.m.}(\mathrm{We_f})=\mathrm{Im}^{-1}(z_\mathrm{m}(\mathrm{We_f}))U_\mathrm{g}/b$, as functions of $\mathrm{We_f}$, representing flow conditions, which are shown in fig. 4.

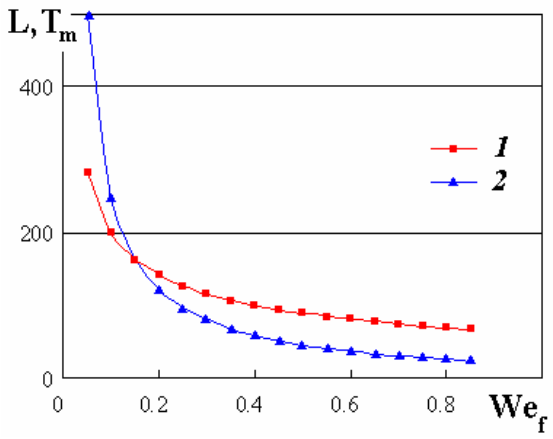

Figure 4 Dependencies $L_\mathrm{m}(\mathrm{We_f})-\boldsymbol{1}$, $T_\mathrm{e.m.}(\mathrm{We_f})-\boldsymbol{2}$

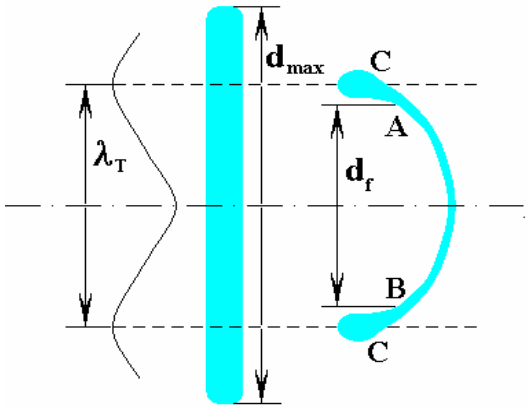

Figure 5 Scheme of bag blowing

The theoretical description of bag and bag-with-a-stamen formation, which was done in [9], [10] and some experimental observations give the possibility to evaluate the bag film volume V_f and the bag film thickness b. Let's hold the scheme of action of unstable aperiodic disturbance λ_T of Taylor type [9], [10]. Near the moment of disturbance transition from linear to non-linear stage a part of liquid layer AB with diameter d_f is formed around axis (fig. 5) by "positive phase", from which bag will be blown afterwards. This volume is equal to $V_\mathrm{f}=\pi d_\mathrm{f}^2\cdot d/4$, where d is the liquid disk thickness. The rest of the liquid volume $V_\mathrm{r}=V_0-V_\mathrm{f}$ is gathered in locations C of "opposite phase" of disturbance, and forms massive rim by the action of surface tension forces.

In this scheme the ratio $V_\mathrm{f}/V_\mathrm{r}$ can be defined by the values of two coefficients of proportionality: k_λ between wavelength and maximum degree of drop deformation, $\lambda_\mathrm{T}=k_\lambda d_\mathrm{max}$, which exceeds to the moment of transition from linear to non-linear stage; and k_f between diameter AB and wavelength, $d_\mathrm{f}=k_\mathrm{f}\lambda_\mathrm{T}$. Values of λ_T are defined by flow conditions, and dependence $\lambda_\mathrm{T}(\mathrm{We_0})$ was calculated in [9], [10]; within the range $\mathrm{We_{0cr.1}}<\mathrm{We_0}<\mathrm{We_{0cr.2}}$ of "bag" mode it can be approximated by the expression: $\lambda_\mathrm{T}=10.4D_\mathrm{max}^{1/3}\mathrm{We}^{-0.58}d_0$. Here $\mathrm{We_{0.cr.1}}\approx 5$ and $\mathrm{We_{0.cr.2}}\approx 32$ are the lower and upper limits for "bag"; $\mathrm{We_0}=\rho_\mathrm{g}U_\infty d_0/\sigma$ is Weber number for parent drop, U_∞ is stream velocity, d_0 is initial drop diameter. Hence, k_λ can be computed by the formula: $k_\lambda=10.4\mathrm{We}_0^{-0.58}D_\mathrm{max}^{-2/3}$. Values of d_max are defined by both drop deformation under aerodynamic forces action and simultaneous action of unstable disturbance, which terminates the former. There are opposite evidences concerning dependency of D_max on $\mathrm{We_0}$: the decreasing, as fig. 4, [1] shows; and increasing, as some experiments [4] show.

The development of aperiodic unstable disturbance of Taylor type was studied experimentally by Lewis [12]. He found, in particular, that the linear stage of exponential growth terminates, when disturbance' amplitude

reaches the value $E \approx 0.4\lambda$; and when $E \approx 0.75\lambda$, the non-linear stage with constant velocity $U_T = 0.239\sqrt{g\lambda_T}$ of gas "fingers" penetration begins. Taking use of photographs only with wave envelopes in order to eliminate influence of channel sides, the coefficient k_f can be roughly estimated as $k_f = 0.8 \div 0.9$. At lower limit $We_{0.cr.1} \approx 5$, when only one half-wave-length works, the coefficient must be twice lesser: $k_f = 0.4 \div 0.5$; so, the dependence $k_f(We)$ can have the approximative linear form: $k_f = 0.45 + (We_0 - 5)/62$.

With these estimations for the values of k_f, k_λ, let's write down expressions for liquid volumes in the bag film $V_f = \pi(k_f\lambda_T/2)^2 d_0 / D_{max}^2 = \pi(k_f k_\lambda)^2 d_0^3/4$, and in the rim $V_r = V_0 - V_f = \pi d_0^3/6 - \pi(k_f k_\lambda)^2 d_0^3/4 = = \pi d_0^3\left(2 - 3(k_f k_\lambda)^2\right)/12$. From the other hand, the liquid volume in bag film is equal to $b \cdot S_{bag}$. The surface area of bag can be estimated visually on fig. 1 as $S_{bag} = \pi d_b^2 \approx k_b \pi d_{max}^2$, where $d_b = k_b d_{max}$ is bag diameter, $k_b \approx 0.7 \div 1.0$. Then, equalizing the two expressions for V_f gives an evaluation for the film thickness:

$$b = \frac{k_f^2 k_\lambda^2}{4k_b}\frac{d_0}{D_{max}^2}. \qquad 5)$$

Let's get some estimations at $d_0 = 705\mu m$, $We_0 = 19.5$, which correspond to the test conditions of fig. 1. Assuming $k_b = 0.9, D_{max} = 3.0$, and taking $k_\lambda(19.5) = 0.89$, $k_f(19.5) = 0.68$, the expression (5) gives $b \approx 0.012 d_0 = 8.1\mu m$, then $We_f = 0.449$, $V_f \approx 0.102 mm^3$. The part of film volume is $V_f = 0.56V_0$ of total liquid volume of drop. The calculated values of $b = 0.0115 d_0$ and of $V_r = 0.44V_0$ agree with those, obtained in experiments [13]: $b = 0.01 d_0$, $V_r = 0.56V_0$. The calculated value of dominant wavelength is $\lambda_{m.th.} = 0.60 d_0 = 425.0\mu m$ while estimation of experimental value by fig. 1 yields $\lambda_{m.ex.} \approx 0.28 d_0$. The discrepancy may be explained by unaccounted gradient flow inside the film due to viscous stresses of air flow on the film surface $y = b$, which may be improved by correction of instability treatment model.

Dynamic process of daughter droplets formation as a result of bag film rupture and their sizes will be described in the next sections.

Dynamics of Liquid Roller

Let us consider infinite plane liquid layer of thickness b, density ρ_l, which was perforated at initial moment $t = 0$ by unstable disturbance of wavelength λ_m, and a round hole of radius $r_0 = k_h \lambda_m$, $k_h \approx 0.25$ appeared as a result. Under action of surface tension forces the liquid at the edge of the layer is gathered into toroidal roller. Left-hand-side vectors of forces, which are opposite to the layer, are not compensated, and a sys-tem of surface tension forces has the resultant force $\vec{F}_{s.t.}$ (fig. 6), which accelerates the roller in radial direction outward the hole. Another force, that counteracts to $\vec{F}_{s.t.}$, is reactive force, $\vec{F}_r$, that arises, when the roller runs with velocity $\vec{U}_{rol}$ against still layer. Accounting for axial symmetry, we will derive the equation of roller motion, which is described by current locations of torus center $x(t)$, its mass center $\xi(t)$ and radius of torus $R(t)$.

In cylindrical coordinate system $ZX\varphi$, where OZ is axis of symmetry, let's cut off elementary volume of torus, the cutting is formed by plane sections $\varphi = \pm\varphi_0/2$ (fig. 7). Let's write down the differential equation of mass centre motion in OX-direction:

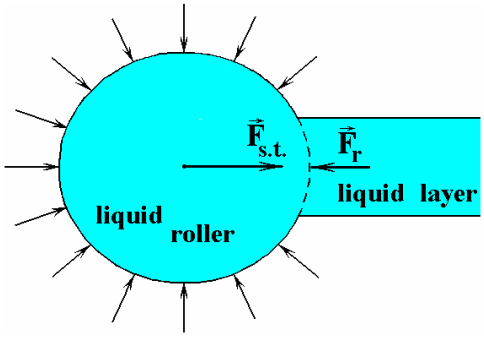

Figure 6 The cross-section of the roller

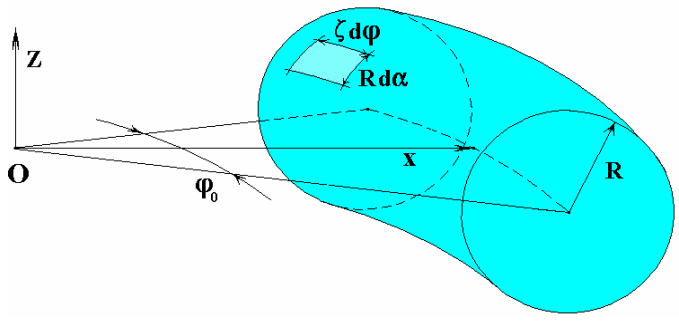

Figure 7 The cut-off element of the roller

$$m\frac{d^2\xi}{dt^2}=F_{\text{s.t.}}+F_{\text{r}}\,. \qquad 6)$$

The expression for surface tension resultant force can be easily obtained by integration along the cut volume surface of the two elementary values, $dF_{\text{s.t.1}}=\frac{\sigma}{R}dS$, $dF_{\text{s.t.2}}=\frac{\sigma}{\zeta}\cos\alpha\, dS$, where R,ζ are the two mean curvature radii, α is polar angle inside cross section. The relations exist between R,x,ξ, which can be easily obtained by geometrical considerations:

$$x(R)=\frac{\pi R^2}{b}-\frac{\sqrt{4R^2-b^2}}{4}-\frac{R^2}{b}arctg\left(\frac{b}{\sqrt{4R^2-b^2}}\right)+\left(\left(\frac{\sqrt{4R^2-b^2}}{4}-\frac{\pi R^2}{b}+\frac{R^2}{b}arctg\left(\frac{b}{\sqrt{4R^2-b^2}}\right)\right)^2-R^2+\frac{b^2}{12}+r_0^2\right)^{0.5},$$

$$\xi(x,R)=\frac{\sin(\varphi_0/2)}{\varphi_0}\frac{1}{2x}\left(4x^2+R^2\right). \qquad 7)$$

Using expressions $\zeta=x+R\cos\alpha$, $dS=R\zeta\, d\alpha\, d\varphi$, and integrating within limits $-\varphi_0/2\le\varphi\le\varphi_0/2$, $arctg\left(\frac{b}{\sqrt{4R^2-b^2}}\right)\le\alpha\le-arctg\left(\frac{b}{\sqrt{4R^2-b^2}}\right)$, we obtain the needed expression:

$$F_{\text{s.t.}}=-\sigma\sin\frac{\varphi_0}{2}\left(4\pi R-\frac{2xb}{R}-\frac{b\sqrt{4R^2-b^2}}{R}-4R\cdot arctg\left(\frac{b}{\sqrt{4R^2-b^2}}\right)\right). \qquad 8)$$

The reactive force is $dF_{\text{r}}=-\frac{d\xi}{dt}\frac{dm}{dt}\cos\varphi d\varphi$, where $m=\pi R^2x\rho_l\varphi_0$, $\frac{dm}{dt}=\pi\rho_l R\left(2x+R\frac{dx}{dR}\right)\frac{dR}{dt}$. By integration inside the cut volume we obtain:

$$F_{\text{r}}=2\pi\rho_l R\left(2x+R\frac{dx}{dR}\right)\left(\frac{\partial\xi}{\partial R}+\frac{\partial\xi}{\partial x}\frac{dx}{dR}\right)\left(\frac{dR}{dt}\right)^2\sin\frac{\varphi_0}{2}, \qquad 9)$$

After the calculation of derivatives with a help of (7), we can substitute (7)–(9) into (6) and obtain the **differential equation of liquid roller motion**:

$$\frac{d^2\tilde{R}}{d\tilde{t}^2}=\frac{F_8-\left(F_9\left(F_3+2F_5F_6+F_4F_6^2+F_2F_7\right)+F_{10}\right)\left(\frac{d\tilde{R}}{d\tilde{t}}\right)^2}{F_9(F_1+F_2F_6)}, \qquad 10)$$

where $\tilde{t}=t/t_{\text{ch.r.}}$ is dimensionless time, $t_{\text{ch.r.}}=\sqrt{\rho_l b^3/\sigma}$ is a characteristic time interval for dynamic process of roller motion, $F_1,\ldots,F_{10}$ are functions of $\tilde{x}=x/b,\tilde{R}=R/b$, which are listed in **Appendix.** Initial value of roller radius $\tilde{R}(0)$ for a given $\tilde{r}_0$ was obtained from the first equation (7) and relation $\tilde{x}(0)=\tilde{r}_0+\tilde{R}(0)$; it has almost the identical values $\tilde{R}(0)\approx0.59$ for all the variants; initial value $d\tilde{R}/d\tilde{t}$ was set to zero. Numerical integration of (10) was carried out with a help of Runge – Kutta procedure of fourth degree of accuracy.

Results and Conclusions

The dynamics of the liquid film after initial perforation was then investigated by means of calculation of roller motion law $\tilde{x}(\tilde{t})$, law of roller radius growth, $\tilde{R}(\tilde{t})$, and simultaneous determination of possibility of dominant disturbance performance, with a help of relationships (2)–(4), (10). When the time $T_{\text{e.m.}}$, needed for e-fold growth of dominant disturbance, was terminated, it was assumed, that the roller is torn off from the liquid film by instability and is scattered onto droplets of radius $\tilde{R}(T_{\text{e.m.}}-0)$, which the roller had that moment. Value $\tilde{x}(\tilde{T}_{\text{e.m.}}-0)-\tilde{R}(\tilde{T}_{\text{e.m.}}-0)$ was then taken as a new value for radius of the hole $\tilde{r}_0(\tilde{T}_{\text{e.m.}}+0)$ and the initial radius of new roller was determined by equation $\tilde{x}(\tilde{T}_{\text{e.m.}}+0)=\tilde{r}_0+\tilde{R}(\tilde{T}_{\text{e.m.}}+0)$ and first equation (7). Thus, the calculations were continued, until, as a result of manifold splashes (their number varied from 29 at $\text{We}_0=8$, to 77 at

$\mathrm{We}_0 = 32$), the volume of torn off droplets exceeded the total volume of liquid in the bag film, V_f, and the process of the film disintegration was assumed to be finished.

The dynamic process of bag disintegration was calculated for water drop in three airstreams with Weber number values of $\mathrm{We}_0 = 8;\ 19.5;\ 32$; mentioned above relationships $k_\mathrm{f}(\mathrm{We}_0)$, $k_\lambda(\mathrm{We}_0)$ were applied, and constant $d_0 = 705\mu m$, $k_\mathrm{b} = 0.9$ were used. The second variant corresponds to test conditions of fig. 1. Some difficulties arose while setting up of a value of a lateral deformation, $D_{\max}$, which drop had at the moment of the dominant disturbance transition from linear to non-linear stage. Figure 4 of [1], gets evidence that the function $D_{\max}(\mathrm{We}_0)$ may exist, having decreasing character. Such tendency is confirmed by the dependence obtained in [10] for critical degree of deformation, $D_{\mathrm{cr}} = 20\mathrm{We}_0^{-4/3} + 0.8$, which is needed for "bag" mode of breakup. Hence, the three variants were calculated with values $D_{\max} = 3.0;\ D_{\max} = 2.5;\ D_{\max} = 2.0$, respectively.

The results are presented in figs. 8, 9 and in the ***Table***. The effect of surface tension forces on the roller growth is essential; indeed, the average diameters of generated daughter droplets d_d are sufficiently greater, than the bag film thickness: $d_{\mathrm{d.a.}1} = 3.94b$, $d_{\mathrm{d.a.}2} = 2.59b$, $d_{\mathrm{d.a.}3} = 1.63b$, for the three variants. These values approximately conform to those seen in fig. 2, b). In each variant the droplet sizes are distributed over the narrow range: $24.8 \le d_{\mathrm{d}1} \le 26.7$, $20.0 \le d_{\mathrm{d}2} \le 22.0$, $23.6 \le d_{\mathrm{d}3} \le 28.1$ (in μm) and are almost monodisperse, as was found in experiment [13]. The average values $d_{\mathrm{d.a.}i}$ are close to experimental value, $d_{\mathrm{d.av.}} = 0.04 d_0$ [13], too.

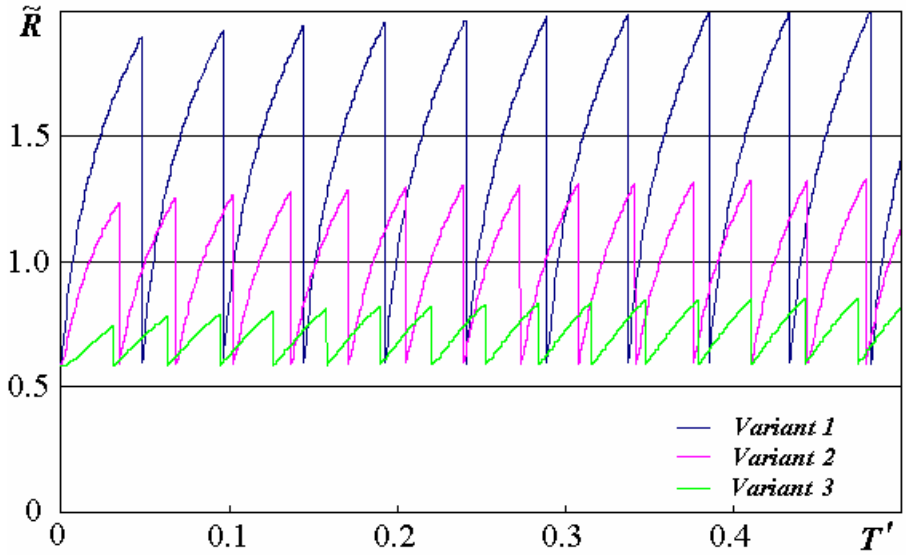

Figure 8 Torus radius histories in dimensionless variables; $T' = t/t_{\mathrm{ch.br.}}$, $t_{\mathrm{ch.br.}} = d_0/\sqrt{\alpha U_\infty}$.

The histories of the liquid torus radius are shown in fig. 8. The rate of radius growth $\dot{\tilde{R}}$ is greatest at the beginning, but it drops quickly under the action of reactive force. Figure 8 shows, that the smaller We_0 is, the greater is the period of roller splashings, and the radii of generated daughter droplets are greater, having some increase in time. The characteristic time scale of parent drop breakup $t_{\mathrm{ch.br.}}$ exposes the partition of the film disintegration period in total drop breakup time $T'_{\mathrm{br}} = 5 \div 6$.

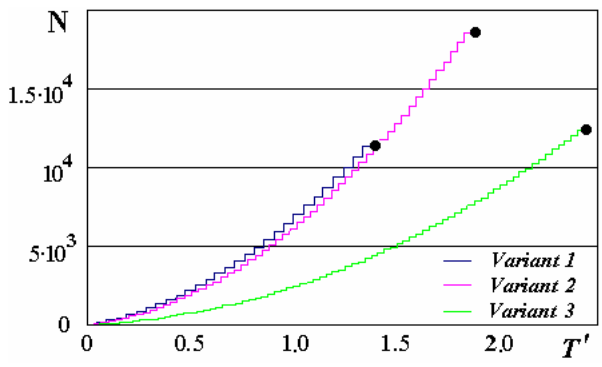

Figure 9 Histories of number of daughter droplets; ● – moment T'_{dis} of final bag disintegration

The histories of the number of generated daughter droplets are given in fig. 9, which shows, that at greater We_0 the disintegration of bag film proceeds slower, due to a thicker bag film. The mass histories of torn off droplets are almost similar to $N(T')$. The mean droplets radii are not mono-

tonic with respect to We_0 under influence of the two opposite factors: they grow due to increase of $D_{\max}$ (via growth of b) and drop with increasing We_0. The same can be said with regard to the period of full disintegration of the bag film t_{dis}.

Table Values of calculated parameters

	We_0	$D_{\max}$	$b, \mu m$	We_{f}	T'_{dis}	$d_{\mathrm{d.a.}}, \mu m$	N_{d}	N_{spl}	V_{f}/V_0
Variant 1	8	3.5	6.54	0.148	1.40	25.73	12066	29	0.61
Variant 2	19.5	3.0	8.11	0.449	1.88	20.96	19230	55	0.56
Variant 3	32	2.5	15.9	1.442	2.43	25.86	12681	77	0.76

The results have shown the weak influence of initial hole radius on the main parameters: as $\tilde{r}_0$ increases from 3 to 30 a final value of $\tilde{R}$ increases only by 30%. Calculated value of velocity of roller motion along film surface is almost the same in the three variants and approximately equals to $d\tilde{x}/d\tilde{t} \approx C$, which in dimensional form is equivalent to $\frac{dx}{dt} \approx C\sqrt{\frac{\alpha d_0}{b\mathrm{We}_0}}U_\infty$ with $C=0.48; C=0.49; C=0.44$ for the three variants. For the test shown in fig. 1 it yields $\approx 1.48 m/\mathrm{sec}$.

Summary

The presented model of bag film disintegration allows to obtain all the main kinetic parameters of the process – sizes of torn off droplets, moments of their tearing off and mass history of formation of aerosol cloud of daughter droplets in the wake of a parent drop. Many of parameters have the influence on the process, and multiparameter analysis is required. Among those the most strong influence has We_0, which decreases $d_{\mathrm{d}}, t_{\mathrm{dis}}$, and $D_{\max}$, which has an opposite effect. This is the reason why at greater We_0 the total film disintegration time t_{dis} is greater for ***variant 3.*** The dependence $D_{\max}(\mathrm{We}_0)$ and more reliable relationships $k_{\mathrm{f}}(\mathrm{We}_0), k_\lambda(\mathrm{We}_0), k_{\mathrm{b}}(\mathrm{We}_0)$ are needed for more accurate evaluations of $b, d_{\mathrm{d}}, T'_{\mathrm{b}}$.

The elaborated model permits to construct models of further evaporation and mixing kinetics of generated aerosol mist.

The final stage of disintegration process – breakup of massive rim, – needs further hypotheses and theoretical investigation.

Appendix

Here we give the expressions for coefficients of eq. 1 as functions of H:

$$A_1 = -(1-\exp(-2H)); \quad A_2 = -2\mathrm{We}_{\mathrm{f}}(1+\exp(-2H)); \quad A_3 = -\mathrm{We}_{\mathrm{f}}^2(1-\exp(-2H)); \quad A_4 = 2\mathrm{We}_{\mathrm{f}}H(1+\exp(-2H));$$

$$A_5 = 2\mathrm{We}_{\mathrm{f}}^2H(1-\exp(-2H)); \quad A_6 = -\mathrm{We}_{\mathrm{f}}^2H^2(1-\exp(-2H)); \quad A_7 = 2H^3(1+\exp(-2H)) - \mathrm{We}_{\mathrm{f}}H^2(1+\exp(-2H));$$

$$A_8 = -2\mathrm{We}_{\mathrm{f}}H^4(1-\exp(-2H)); \quad A_9 = -H^6(1-\exp(-2H)) + \mathrm{We}_{\mathrm{f}}H^5(1-\exp(-2H)).$$

Here we give the expressions for coefficients of eq. 4 as functions of H_{m}:

$$W_1 = 4H_{\mathrm{m}}^3(3H_{\mathrm{m}} - \mathrm{We}_{\mathrm{f}})(2H_{\mathrm{m}} - \mathrm{We}_{\mathrm{f}})(1+\exp(-2H_{\mathrm{m}}))^2 - 4H_{\mathrm{m}}^4(2H_{\mathrm{m}} - \mathrm{We}_{\mathrm{f}})^2(1+\exp(-2H_{\mathrm{m}}))\exp(-2H_{\mathrm{m}}) - \\ -4H_{\mathrm{m}}^4(6H_{\mathrm{m}} - 5\mathrm{We}_{\mathrm{f}})(1-\exp(-2H_{\mathrm{m}}))^2;$$

$$W_2 = H_{\mathrm{m}}^2\sqrt{(2H_{\mathrm{m}} - \mathrm{We}_{\mathrm{f}})^2(1+\exp(-2H_{\mathrm{m}}))^2 - 4H_{\mathrm{m}}(H_{\mathrm{m}} - \mathrm{We}_{\mathrm{f}})(1-\exp(-2H_{\mathrm{m}}))^2};$$

$$W_3 = 2H_{\mathrm{m}}(3H_{\mathrm{m}} - \mathrm{We}_{\mathrm{f}})(1+\exp(-2H_{\mathrm{m}})) + 2H_{\mathrm{m}}^2(2H_{\mathrm{m}} - \mathrm{We}_{\mathrm{f}})\exp(-2H_{\mathrm{m}})$$

Here we give the expressions for coefficients of eq. 10 as functions of $\tilde{x}$, $\tilde{R}$:

$$F_1=\frac{\partial\tilde{\xi}}{\partial\tilde{R}}=\frac{\tilde{R}}{\tilde{x}};\quad F_2=\frac{\partial\tilde{\xi}}{\partial\tilde{x}}=\frac{1}{2}\left(4-F_1^2\right);\quad F_3=\frac{\partial^2\tilde{\xi}}{\partial\tilde{R}^2}=\frac{1}{\tilde{x}};\quad F_4=\frac{\partial^2\tilde{\xi}}{\partial\tilde{x}\partial\tilde{R}}=\frac{\tilde{R}^2}{\tilde{x}^3};\quad F_5=\frac{\partial^2\tilde{\xi}}{\partial\tilde{x}^2}=-\frac{\tilde{R}}{\tilde{x}^2};$$

$$F_6=\frac{d\tilde{x}}{d\tilde{R}}=2\pi\tilde{R}-2\tilde{R}arctg\left(\frac{1}{\sqrt{4\tilde{R}^2-1}}\right)+\frac{\left(\frac{\sqrt{4\tilde{R}^2-1}}{4}-\pi\tilde{R}^2+\tilde{R}^2arctg\left(\frac{1}{\sqrt{4\tilde{R}^2-1}}\right)\right)\left(2\tilde{R}arctg\left(\frac{1}{\sqrt{4\tilde{R}^2-1}}\right)-2\pi\tilde{R}\right)-\tilde{R}}{\sqrt{\left(\frac{\sqrt{4\tilde{R}^2-1}}{4}-\pi\tilde{R}^2+\tilde{R}^2arctg\left(\frac{1}{\sqrt{4\tilde{R}^2-1}}\right)\right)^2-\tilde{R}^2+\frac{1}{12}+\tilde{r}_0^2}};$$

$$F_7=\frac{d^2\tilde{x}}{d\tilde{R}^2}=2\pi+\frac{2}{\sqrt{4\tilde{R}^2-1}}-2arctg\left(\frac{1}{\sqrt{4\tilde{R}^2-1}}\right)+$$
$$+\frac{\left(2\tilde{R}arctg\left(\frac{1}{\sqrt{4\tilde{R}^2-1}}\right)-2\pi\tilde{R}\right)^2+\left(\frac{\sqrt{4\tilde{R}^2-1}}{4}-\pi\tilde{R}^2+\tilde{R}^2arctg\left(\frac{1}{\sqrt{4\tilde{R}^2-1}}\right)\right)\left(2arctg\left(\frac{1}{\sqrt{4\tilde{R}^2-1}}\right)-2\pi-\frac{2}{\sqrt{4\tilde{R}^2-1}}\right)-1}{\sqrt{\left(\frac{\sqrt{4\tilde{R}^2-1}}{4}-\pi\tilde{R}^2+\tilde{R}^2arctg\left(\frac{1}{\sqrt{4\tilde{R}^2-1}}\right)\right)^2-\tilde{R}^2+\frac{1}{12}+\tilde{r}_0^2}}-$$
$$-\frac{\left(\left(\frac{\sqrt{4\tilde{R}^2-1}}{4}-\pi\tilde{R}^2+\tilde{R}^2arctg\left(\frac{1}{\sqrt{4\tilde{R}^2-1}}\right)\right)\left(2\tilde{R}arctg\left(\frac{1}{\sqrt{4\tilde{R}^2-1}}\right)-2\pi\tilde{R}\right)\right)^2}{\left(\sqrt{\left(\frac{\sqrt{4\tilde{R}^2-1}}{4}-\pi\tilde{R}^2+\tilde{R}^2arctg\left(\frac{1}{\sqrt{4\tilde{R}^2-1}}\right)\right)^2-\tilde{R}^2+\frac{1}{12}+\tilde{r}_0^2}\right)^3};$$

$$F_8=\tilde{F}_{\text{s.t.}}=\frac{2\tilde{x}}{\tilde{R}}-4\pi\tilde{R}+\frac{\sqrt{4\tilde{R}^2-1}}{\tilde{R}}+4\tilde{R}arctg\left(\frac{1}{\sqrt{4\tilde{R}^2-1}}\right);\quad F_9=\pi\tilde{R}^2\tilde{x};\quad F_{10}=\tilde{F}_{\text{r}}=2\pi\tilde{R}\left(2\tilde{x}+\tilde{R}F_6\right)\left(F_1+F_2F_6\right);$$

References

[1] Hanson A. R., Domich E. Y. and Adams H. S., *Physics of Fluids* **6**: 1070–1080 (1963)

[2] Reinecke W. G. and Waldman G.D., *Shock layer shattering of cloud drops in reentry flight,* American Institute of Aeronautics and Astronautics Paper 152: 22 (1975)

[3] Gelfand B.E., Gubin S.A. and Kogarko S.M. *Journal of Engineering Physics and Thermophysics* **27**: 877-882 (1974).

[4] Hsiang L.-P., Faeth G. M. *International Journal of Multiphase Flow* **18**: 635-652 (1992)

[5] Gordon G. D. *Journal of Applied Physics* **30**: 1759–1761 (1959)

[6] Buzukov A. A. *Journal of Applied Mechanics and Technical Physics* **4**: 154-158 (1963)

[7] Schmehl R., *18th Annual Conference on Liquid Atomization and Spray Systems*, Zaragoza, Spain: 495-501 (2002)

[8] O'Brian V., *Journal of Meteorology* **18**: 549–552 (1961)

[9] Girin A. G., *Journal of Engineering Physics and Thermophysics* **48**: 560-564 (1985)

[10] Girin A. G. *12th ICLASS 2012*, Heidelberg, Germany, Sept. 2-6 : # 1225 (2012)

[11] Zhao H., Liu H.-F., Cao X.-K., Li W.-F. and Xu J.-L. *International Journal of Multiphase Flow* **37**: 530-534 (2011)

[12] Lewis D.J. *Proceedings of Royal Society of London, Ser. A* **202**: 81-96 (1950)

[13] Chou W.-H., Hsiang L.-P. and Faeth G. M. *Dynamics of drop deformation and formation during secondary breakup in the bag breakup regime,* AIAA Paper 97-0797: (1997)